

AD-A130 299

EISCAT ELECTRON DENSITY STUDIES(U) LANCASTER UNIV  
BAILRIGG (ENGLAND) DEPT OF ENVIRONMENTAL SCIENCES  
S C KIRKWOOD ET AL. 01 MAY 83 AFGL-TR-83-0165

1/1

UNCLASSIFIED

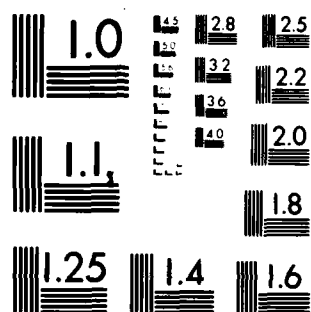
AFOSR-83-0054

F/G 20/9

NL

|  |  |  |  |  |  |  |  |  |  |  |  |  |  |
|--|--|--|--|--|--|--|--|--|--|--|--|--|--|
|  |  |  |  |  |  |  |  |  |  |  |  |  |  |
|  |  |  |  |  |  |  |  |  |  |  |  |  |  |
|  |  |  |  |  |  |  |  |  |  |  |  |  |  |
|  |  |  |  |  |  |  |  |  |  |  |  |  |  |
|  |  |  |  |  |  |  |  |  |  |  |  |  |  |

END  
DATE  
FILMED  
DTIC



MICROCOPY RESOLUTION TEST CHART  
NATIONAL BUREAU OF STANDARDS-1963-A

00A 130.99

DTIC FILE COPY

3

Unclassified

SECURITY CLASSIFICATION OF THIS PAGE (When Data Entered)

| REPORT DOCUMENTATION PAGE  |                                    | READ INSTRUCTIONS<br>BEFORE COMPLETING FORM                                |
|--|------------------------------------|--|
| 1. REPORT NUMBER<br>AFGL-TR-83-0165  | 2. GOVT ACCESSION NO.<br>AD-A30274 | 3. RECIPIENT'S CATALOG NUMBER  |
| 4. TITLE (and Subtitle)<br>EISCAT ELECTRON DENSITY STUDIES<br>(Second Year)  |                                    | 5. TYPE OF REPORT & PERIOD COVERED<br>Final, 1 May 1982-30 April 1983      |
| 7. AUTHOR(s)<br>S.C. Kirkwood and J.K. Hargreaves  |                                    | 6. PERFORMING ORG. REPORT NUMBER   |
| 9. PERFORMING ORGANIZATION NAME AND ADDRESS<br>Environmental Sciences Dept., University of<br>Lancaster, Bailrigg, Lancaster, England.   |                                    | 8. CONTRACT OR GRANT NUMBER(s)<br>AFOSR-83-0054                            |
| 11. CONTROLLING OFFICE NAME AND ADDRESS<br>Air Force Geophysics Laboratory<br>Hanscom AFB, Massachusetts 01731<br>Monitor/John A. Klobuchar/IHP  |                                    | 10. PROGRAM ELEMENT, PROJECT, TASK<br>AREA & WORK UNIT NUMBERS<br>2310G6AC |
| 14. MONITORING AGENCY NAME & ADDRESS (if different from Controlling Office)<br>EOARD/ING, Box 14, FPO, New York 09510.   |                                    | 12. REPORT DATE<br>1 May 1983  |
|  |                                    | 13. NUMBER OF PAGES<br>46  |
|  |                                    | 15. SECURITY CLASS. (of this report)<br>Unclassified                       |
|  |                                    | 15a. DECLASSIFICATION/DOWNGRADING<br>SCHEDULE                              |
| 16. DISTRIBUTION STATEMENT (of this Report)<br>Approved for public release; distribution unlimited.  |                                    |  |
| 17. DISTRIBUTION STATEMENT (of the abstract entered in Block 20, if different from Report)   |                                    |  |
| 18. SUPPLEMENTARY NOTES  |                                    |  |
| 19. KEY WORDS (Continue on reverse side if necessary and identify by block number)<br>Incoherent scatter radar; auroral zone; ionospheric F region; small-scale<br>plasma irregularities.  |                                    |  |
| 20. ABSTRACT (Continue on reverse side if necessary and identify by block number)<br>Operational details and first results of a program to study irregular electron<br>density structure in the auroral F-region using the EISCAT incoherent-scatter<br>radar are presented. Large amplitude, localised, electron density enhancements<br>are observed in active, night-time conditions. Two types of large-scale<br>enhancement are seen: one with large amplitudes in the E and lower F-region,<br>with amplitudes decreasing rapidly with further increase in altitude, the<br>P.T.O. |                                    |  |

DTIC  
ELECTE  
JUL 13 1983  
S D

DD FORM 1473 1 JAN 73 EDITION OF 1 NOV 65 IS OBSOLETE

Unclassified

SECURITY CLASSIFICATION OF THIS PAGE (When Data Entered)


8-3 07 12

175

Unclassified

SECURITY CLASSIFICATION OF THIS PAGE(When Data Entered)

other confined to the F-region with largest amplitudes on the topside. Evidence for intermediate scale structuring associated with precipitation, in some instances, and with probable formation by plasma instabilities in others, is also presented.



Unclassified

SECURITY CLASSIFICATION OF THIS PAGE(When Data Entered)

Grant Number AFOSR 83-0054

EISCAT ELECTRON DENSITY STUDIES  
(Second Year)

S.C. Kirkwood and J.K. Hargreaves,  
Environmental Sciences Department,  
University of Lancaster,  
Lancaster. LA1 4YQ  
England.

1 May 1983

Final Report 1 May 1982 - 30 April 1983

|                    |                                     |
|--------------------|-------------------------------------|
| Accession For      |                                     |
| NTIS GRA&I         | <input checked="" type="checkbox"/> |
| DTIC TAB           | <input type="checkbox"/>            |
| Unannounced        | <input type="checkbox"/>            |
| Justification      |                                     |
| By                 |                                     |
| Distribution/      |                                     |
| Availability Codes |                                     |
| Avail and/or       |                                     |
| Dist               | pecial                              |
| A                  |                                     |

Prepared for AFGL/PHY, Hanscomb AFB, MA 01731,  
USA and European Office of Aerospace Research  
and Development, London, England.



07 12 175

## Introduction

This report describes the first results of a research programme aimed at studying irregularities in electron density in the auroral F-region, using the EISCAT incoherent scatter radar.

A great deal is already known about F-region irregularities from ground-based radio wave observations (scintillation studies) and from in situ measurements made by satellites and rockets. These have provided statistical information on geographic, time of day, seasonal and magnetic activity dependence of irregularity occurrence (summarized in Table 1), on their scale size distribution, and some studies of field alignment and shape have been made (Fremouw and Lansinger, 1981; Rino and Vickrey, 1982; Livingston et al., 1982). Measurements using radio waves are however indirect, depending on diffraction of the waves by the irregularity pattern. In general effects may have occurred anywhere along the wave path, so the height of scintillation producing irregularities, in particular, is hard to measure. Satellites and rockets measure only along a fixed path, so space and time variations cannot be separated. An incoherent scatter radar can measure electron density directly for long periods of time, at several heights simultaneously, and at several geographic locations successively, and so should be able to provide direct measurements of heights, shapes, sizes, alignments, lifetimes and drifts as well as adding more statistical information on irregularity occurrence. Such information would be invaluable in evaluating the various theories on how irregularities are formed. Indeed, recent studies using the Chatanika radar have identified large-scale (tens of kilometres) electron density enhancements or 'blobs', with scintillation producing zones apparently associated with the edges of the 'blobs' (Muldrew and Vickrey, 1982). Much work remains to be done in determining the detailed structure and dynamics of these 'blobs'.

Table 1 High latitude irregularity characteristics. Note that upper limit to altitude range is upper limit of observations, not necessarily limit of irregularities. Except where marked, information is from Clark and Raitt, 1976.

| Zone             | Location   | Average Intensity ( $\Delta N/N$ ) RMS | Occurrence  | Possible Production Mechanism   |
|------------------|--|--|---|---|
| polar zone       | >72°-84°, midnight<br>>65°-82°, noon   | moderate<br>- strong<br>(6-10%)        | all times, all altitudes<br>(400 <sup>2</sup> -3500 <sup>1</sup> km)  | poleward motion of irregularities generated in auroral zone   |
| auroral zone     | <sup>3</sup> varies with magnetic activity<br>64°-74°N, midnight<br>72°-74°N, noon<br>for Kp ~ 3 | strong<br>(8-10%)                      | all times, all altitudes (350 <sup>2</sup> -3500 <sup>1</sup> km)<br>Increasing intensity and equatorward movement of boundary with increasing Kp | 1) particle precipitation<br>2) electrostatic turbulence<br>3) <sup>4</sup> plasma instabilities  |
| sub auroral zone | between 50°-60° and 64°N, midnight   | moderate<br>(4-6%)                     | only at night, all altitudes (300 <sup>2</sup> -3500 <sup>1</sup> km)   | 1) <sup>4</sup> equatorward motion from creation in auroral zone<br>2) magnetospheric heat conduction<br>3) heat transfer from ring current<br>4) heating effect of conjugate photo electrons in winter |

<sup>1</sup>Phelps, A.D.R., Sagalyn, R.C., 1976  
<sup>2</sup>Frihagen, J., 1970

<sup>3</sup>Sandford, B.P. 1970

<sup>4</sup>Fejer, B.G., Kelley, M.C., 1980

The major restrictions in using incoherent scatter data for this purpose are the spatial resolution and measurement accuracy. These are determined by the details of the radar facility - beam width and power in particular - and in the case of EISCAT will probably restrict spatial resolution to about 5 km irregularity scale size at 300 km altitude. While this is not adequate to resolve scintillation producing irregularities (tens to hundreds of meters scale-size), it should be good enough to study the structuring of these large-scale electron density enhancements, which is very probably the source of the smaller-scale irregularities.

Relevant details of the EISCAT hardware are listed in Table 2. The system transmits according to some predetermined pulse scheme and pointing sequence from Tromso and records the scattered signal at Tromso, Kiruna and Sodankyla. The scattered wave contains information on electron density, temperature and drift, and on ion temperature. The remote sites are generally used to determine 3-D drifts, the Tromso receiver being used for the other measurements.

Three types of irregularity measurement will be possible:

#### 2-D measurements

If the Tromso antenna points in a fixed direction we will be able to derive statistical information on the time and height variation of irregularity amplitudes and occurrence.

#### 3-D measurements

If measurements are made at a series of positions (e.g. latitude or longitude scan), for several integration periods at each position, we will be able to derive the same information as in the 2-D case and any statistical variation with position in addition.

#### 4-D measurements

If we used rapid latitude and longitude scanning with closely spaced measurements, one integration period at each point, we should get a complete



Table 2.

Details of EISCAT System (VHF)

|             |  |   |
|-------------|--|---|
| Location    | Tronso ( $T_x, R_x$ )  | 66.6°N, 104.9°E (corrected geomagnetic) |
|             | Kiruna ( $R_x$ )   | 64.9°N, 104.2°E                         |
|             | Sodankyla ( $R_x$ )  | 63.9°N, 108.5°E                         |
| Antennae    | Diameter 32 m  |   |
|             | Half-power beam width 0.6°   |   |
|             | Steerability:  |   |
|             | elevation  | 10° - 90°                               |
|             | azimuth  | ± 270°                                  |
|             | Maximum slewing rate   | 80°/minute                              |
| Transmitter | Frequency 933.5 ± 2.5  |   |
|             | (choice of 8 frequencies in 0.5 MHz steps)   |   |
|             | Peak power output 2 MW (0.5 MW only up to March 1981 generally 1.0 MW only up to March 1983) |   |
|             | Average power 250 kW   |   |
|             | Pulse repetition rate  | 0 - 1000 Hz                             |
|             | Pulse length   | 10 µsec - 10 msec, variable             |

4-D picture at least over a small range of latitude and longitude.

These three types of measurement will be catered for by EISCAT "Common Programs" (2-D, 3-D) and by purpose designed "Special Programs" (4-D).

Common programs are run at times decided at EISCAT HQ, generally during one 24 hour period each week, on Tuesday/Wednesday. Time is allocated for Special programs during specific 'campaign' periods, of about 2 weeks duration, the precise time being chosen according to any special conditions required for the experiment.

#### Eiscat operations up to March 1983

##### Common Programs

Common program runs were made between August 1981 and January 1982 with the transmitter operating at about 500 kW, and were restarted in April 1982 at about 1 MW, occasionally higher. Klystron failure took the system out of service from the end of August to late November 1982. The system operated, with frequent breakdowns until mid-January 1983, when it was again taken out of service for investigation of the recurrent faults.

The actual runs made are listed in Table 3 from which it can be seen that 34 runs of about 24 hours duration have been made. A description of the common programs, based on details given in the EISCAT annual report for 1981, follows.

##### a) Common Programme Zero

CP 0 is a very simple programme designed to give continuous measurements of electron density, electron and ion temperatures and electric fields in the F-region.

All three antennas are fixed: the Tromsø beam set parallel to the magnetic field line and the remote antennas pointing to a fixed height. Two pulses are transmitted. A short pulse is used to give a power profile which can be converted into an electron density profile with height resolution of  $\sim 10$  km. A longer pulse gives profiles of electron density, electron and

ion temperatures and plasma velocity with height resolution of  $\sim 50$  km. The longer pulse also provides an echo for the remote stations which observe a common scattering volume at a height of 300 km.

b) Common Programme One

CP 1 is similar to CP 0 but includes extensive measurements in the E-region.

The Tromsø beam is again set parallel to the field line but the remote antennas scan up and down so that they can measure plasma velocity at a number of heights.

In 1981 and 1982 full frequency agility was not available and so CP-1, a simplified version of CP 1, was run. In this programme a single long pulse was transmitted. This gave profiles of electron density, electron and ion temperature and plasma velocity over the height range 200-800 km with height resolution of  $\sim 75$  km. The remote antennas made measurements at 110, 120, 130, 140, 300 and 700 km.

c) Common Programme Two

In CP 2 the Tromsø beam points in sequence in three different directions so that it is possible to distinguish time- and space-variations, as for example in observations of atmospheric gravity waves.

A simple form of this programme has already been run as CP-2. The three antennas move in a cycle of 6 minutes pointing to the vertices of a right-angled triangle at a height of 300 km. (The positions are at 69.2 N, 19.2 E; 68.4 N, 19.2 E; 68.4 N, 21.1 E at 300 km altitude). The same pulse scheme is used as in CP 0.

d) Common Programme Three

CP 3 is designed to make ionospheric measurements over a wide range of L values. Two versions of CP 3 have been run.

CP-3 (Simple) was developed for collaboration with GEOS. The aim was a latitude scan passing through the GEOS field line with a cycle time of

6 minutes. The mode used was very similar to CP-2 with three pointing directions in the Tromsø meridian at elevations  $62^{\circ}$ ,  $77^{\circ}$  and  $92^{\circ}$ .

The full version of CP 3 was developed for collaboration with MITHRAS and follows a 16-position trajectory which runs perpendicular to the L-shells between latitudes  $74.25^{\circ}\text{N}$  and  $64.25^{\circ}\text{N}$ . The cycle time is 30 minutes.

#### Lancaster University Special Programs

A high-time-resolution, rapid scanning program has been developed specifically to look at small scale variations in electron density. The aim is to scan rapidly back and forward through a structured region, measuring the electron density variations. Tristatic drift measurements every half-hour or so made with the beam stationary should allow us to determine the direction of drift of any structure and so we can resolve a 3-D picture of its morphology. Initial restrictions imposed mainly by the EISCAT software system meant that the scan speed is not as high as we would like. However, this may improve in the near future.

Runs of our special program were attempted in December 1981, June 1982, September 1982 and November/December 1982. Details are as follows:

December 1981:

50-position azimuth and elevation scans (4 of each) in a cross pattern, centred on the magnetic field direction, position spacing 2 km (el-scan), 0.5 km (az-scan) at 300 km range, plus measurements for 2 minutes each half-hour with beam stationary, parallel to magnetic field. Pre-integration time 4 seconds.

pulses  $1 \times 250 \mu\text{s}$ , power  $\sim 500 \text{ kW}$

cycle time 400 secs for each individual scan, 1 hour for complete sequence

Table 3: Common Programme Observations

| Date        | Start (UT) | Stop (UT) | Mode            |
|-------------|------------|-----------|-----------------|
| 81 09 16/17 | 0902       | 0715      | CP-1            |
| 81 09 23/24 | 0930       | 0800      | CP-1            |
| 81 09 30/01 | 1130       | 0900      | CP-1            |
| 81 10 02    | 0825       | 1055      | CP-1            |
| 81 10 06/08 | 2200       | 0900      | CP-1            |
| 81 10 14/15 | 1415       | 0900      | CP-1            |
| 81 10 21/22 | 0910       | 0900      | CP 0            |
| 81 10 25/26 | 1630       | 0900      | CP 0            |
| 81 11 04/05 | 0930       | 0900      | CP 0            |
| 81 11 11    | 0900       | 1450      | CP 0            |
| 81 11 18/19 | 0900       | 0900      | CP 0            |
| 81 11 25/26 | 0900       | 0840      | CP 2            |
| 81 11 29/30 | 1000       | 1000      | CP-3            |
| 81 12 08/09 | 1500       | 2020      | CP-3 (Extended) |
| 81 12 15/16 | 1500       | 1940      | CP-3            |
| 82 01 19/20 | 1500       | 2300      | CP-3            |
| 82 01 26/27 | 1500       | 2300      | CP-3            |
| 82 01 31/01 | 1000       | 1000      | CP-3            |
| 82 04 14/15 | 1300       | 0835      | CP 0            |
| 82 04 21/22 | 1000       | 1300      | CP-2            |
| 82 04 25/26 | 1210       | 1000      | CP 3            |
| 82 05 9/10  | 1018       | 1003      | CP 0            |
| 82 05 12/13 | 1756       | 2356      | CP 3            |

| Date        | Start (UT) | Stop (UT) | Mode |
|-------------|------------|-----------|------|
| 82 05 18/19 | 1630       | 2300      | CP-2 |
| 82 05 26/27 | 1000       | 1000      | CP 3 |
| 82 06 02/03 | 1000       | 1000      | CP 0 |
| 82 06 06/07 | 0958       | 1200      | CP-2 |
| 82 06 16/17 | 1100       | 1100      | CP 3 |
| 82 07 07/08 | 1058       | 1115      | CP-2 |
| 82 07 26    | 1200       | 1328      | CP 3 |
| 82 07 27    | 0000       | 1342      | CP 3 |
| 82 07 27/28 | 2315       | 1355      | CP 3 |
| 82 07 31    | 0000       | 1352      | CP 3 |
| 82 08 01    | 1200       | 1358      | CP 3 |
| 82 08 04/5  | 1200       | 0945      | CP-2 |
| 82 08 11    | 1000       | 2319      | CP 0 |
| 82 08 12    | 0115       | 1000      | CP 0 |
| 82 08 17/18 | 1100       | 0857      | CP-2 |
| 82 11 24    | 1412       | 1750      | CP 0 |
| 82 11 25/26 | 1000       | 1000      | CP 0 |
| 82 11 30/01 | 1000       | 1000      | CP 0 |
| 83 01 09/10 | ?          | ?         | CP 0 |

run 1500-1700 UT on 17 December 1981. Further time was allocated but magnetic conditions were too quiet and ambient electron density too low for worthwhile measurements.

June 1982:

Same scanning sequence as in December 1981

pulses 2 x 250  $\mu$ s, power  $\sim$  1 MW

run 1100-1300 UT on 03 June 1982. Further time was not allocated on this occasion.

September 1982:

Several hours allocated, but not used as transmitter was out of service.

November/December 1982:

64-position azimuth and elevation scans (4 of each), in a cross pattern centred on the magnetic field direction, with position spacing 2 km (el-scan), 0.5 km (az-scan) at 300 km range, plus measurements with beam stationary, parallel to the magnetic field for  $\sim$  8 minutes every  $\sim$  45 minutes. Pre-integration time 4 seconds.

pulses 3 x 250  $\mu$ s, 1 x 50  $\mu$ s, power  $\sim$  800 kW

cycle time 512 secs for each individual scan, 96 minutes for complete sequence

run 2115-2251, 2300-0036 UT on 29-30 November 1982.

A further 10 hours were allocated but not used because of hardware failures.

The original intention in this special program was to aim for the smallest scale-size which could be resolved, hence the short ( $\sim 1^\circ$  of latitude) scans, with closely spaced measurements. Developments during the first year were therefore mainly concerned with improving the signal/noise (using three pulses at different frequencies). However, it has become evident that conditions in the E-region can affect the irregular structure in

the F-region (Vickrey and Kelley, 1982; Kelley et al. 1982) so a power-profile through the E-region was also introduced (but the amplifier in this channel was faulty in Nov. 1982). It has further become clear that structuring on large scale-sizes (100's of kilometres) also plays an important role. A new program has been developed which includes quasi-continuous elevation scans, covering  $\sim 4^\circ$  of latitude to north and south in 2 minute scans, before and after the short, fine resolution scans, in order to look at the fine scale structure in the context of the larger-scale structure. This program was scheduled to run in January 1983, but has been postponed until summer 1983 because of Eiscat hardware problems.

#### Data Analysis Techniques

##### Standard data reduction

It is standard practice to derive the ionospheric parameters electron density ( $N_e$ ), ion temperature ( $T_e$ ) and ion composition, electron temperature ( $T_e$ ) and ion drift velocity ( $V_i$ ) from the size and shape of the spectrum of the scattered signal, and its doppler shift. A computer program which derives these parameters by iterative fitting of model acfs (auto-correlation function, the fourier transform of the spectrum) has been developed by EISCAT staff, principally by Johan Silen, and a copy of this program has been implemented on the UK Science and Engineering Research Council computers by the UK EISCAT group. For the present study, this program has been used to derive  $N_e$ ,  $T_e$ ,  $T_i$  and  $V_i$ , for an assumed fixed ion composition in the F-region (of 100%  $O^+$ ). This usually requires post-integration of the data to 2 or more minutes, so as to ensure clean enough acfs. Since the F-region plasma generally drifts at up to 1 km/s, this can limit the spatial resolution of structure to 120 km. Fortunately drifts are usually rather lower, of the order of a few hundreds m/s, so the resolution attainable is  $\sim 30$  km. The  $V_i$  determined for signals received at each of the three EISCAT

sites let us derive the convection,  $T_e$  and  $T_i$  are indicators of precipitation, and possibly of the age of electron density enhancements (the closer  $T_e$  is to  $T_i$ , in an enhanced region compared to a depleted region, the longer the enhancement may have had to approach equilibrium). Determinations of  $N_e$  show directly whether there are regions of enhancement and depletion, at least at these large scale sizes ( $> 30$  km). There have been considerable doubts about the accuracy of the analysis program used to derive these parameters, particularly in its fitting of  $V_i$ , but it is now thought that the latest version (March 1983) of the program is substantially correct (it fits synthetic acfs correctly, at least for  $T_e, T_i < 3000$  K, R.B. Horne, private communication). However, there are good reasons to believe that the uncertainty estimates, calculated by the program according to how closely the model acf fits the measured one, are substantially underestimated.

Figure 1 shows a comparison of  $N_e, T_e, T_i$  and  $V_i$  profiles, determined using the analysis program, for three different data sets, each recorded at exactly the same time using three different radar frequencies (this data is from the Lancaster University special program run on 29 November 1982). The signal from the third radar frequency in this experiment was artificially shifted to higher frequency (by 2kHz), primarily to give a calibration for the sign of the ionospheric doppler shift. This shift should correspond to a  $V_i$  of 320 m/s, which has been subtracted before plotting the  $V_i$  in Figure 1.

The (arbitrary) scaling factors for the electron density have been chosen to give the closest agreement for the middle time interval.

The error bars plotted are the uncertainty estimates calculated by the analysis program ( $\sigma_c$ ). It is evident that the profiles vary, between the three frequencies, by substantially more than the uncertainty estimates. This is quantified in Figure 2, which shows scatter plots of the observed variations between measurements at different frequencies ( $\sigma_M$ ) vs. the



calculated uncertainties ( $\sigma_c$ ). There is no scatter plot for  $N_e$  as there seem to be systematic discrepancies between the profiles at the earliest and latest times. This is discussed more fully below.

If the  $\sigma_c$  were accurate, then  $\sim 70\%$  of the points in the scatter plots would lie below the solid lines  $\sigma_M = \sigma_c$ . They clearly do not and better estimates of uncertainty would seem to be represented by the dashed lines,  $\sigma_M = 2.5 \sigma_c$  for  $T_e$ ,  $T_i$  and  $\sigma_M = 7 \sigma_c$  for  $N_e$ . The reasons for these discrepancies are not understood but it is possible that different and time-varying distortions of the signals in the different receiver channels, which are not fully accounted for in the analysis, may be responsible. This is supported by the observation that in several cases a profile for one frequency is displaced systematically, rather than randomly, relative to the others at a particular time.

Electron density is determined by applying a correction factor  $(1 + T_e/T_i)$  to the measured power returned from the ionosphere so that the uncertainties in  $T_e$  and  $T_i$  should be the major source of uncertainty in  $N_e$ , at least where long integrations are used, as here, so that the signal and background levels are accurately known. The formula  $\sigma_m \approx 2.5 \sigma_c$  should therefore apply for  $N_e$  also. However, the systematic differences between  $N_e$  profiles at 2115-2123 and 2243-2251, compared to those at 2159-2207 cannot be explained by the differences in  $T_e$  and  $T_i$ . There are differences in the relative powers at the 3 frequencies. This could only happen if the gains in the receiver channels vary or, more likely, if the relative powers transmitted at the 3 frequencies vary. As only the average power is monitored, this cannot be checked from the recorded data. It cannot generally be compensated by averaging over the transmitted frequencies as often there is only one frequency used for the range-profile acf's, while other frequencies are used for close-range power profiles and/or remote-site single-range measurements.

The uncertainties in  $T_e$  and  $T_i$  determination will not seriously affect our studies of irregular structure as we will usually be looking for large variations in these parameters. The uncertainties in velocity determination are more serious as accurate velocities are needed if we want to determine the details of 3D structure and of dynamic conditions. However, it may be possible to improve these determinations by using a different fitting technique and this should be investigated. The uncertainties in  $N_e$ , particularly the apparent variations in relative powers certainly require further investigations. If variations in receiver gain can be ruled out then only data where a single radar frequency was transmitted, or where corresponding data were recorded for all frequencies transmitted, can be used for accurate electron density variation studies, until such time as transmitted power is monitored separately for the different frequencies.

On the positive side, it has been possible to check absolutely the accuracy of the velocity fitting procedure by observing the velocity difference derived in the presence of the artificial doppler shift. A histogram of this difference, for the same data sets used above, is shown in Figure 3, the solid line being all those data values where  $\sigma_c < 4 \text{ m/s}$  ( $\bar{\sigma}_c = 2 \text{ m/s}$ ), the dashed line corresponds to values for which  $\sigma_c < 15 \text{ m/s}$  ( $\bar{\sigma}_c = 5 \text{ m/s}$ ). The mean value of the difference found is  $318 \pm 16 \text{ m/s}$  for the  $\sigma_c < 4 \text{ m/s}$  data, or  $314 \pm 30 \text{ m/s}$  for the  $\sigma_c < 15 \text{ m/s}$  data. These are close to the correct value of  $320 \text{ m/s}$  and the standard deviations are close to what we would expect from the discussion above - i.e. about  $7 \bar{\sigma}_c$ .

#### High time-resolution reduction

The standard reduction described above gives us a picture of large scale variations in the ionosphere and a determination of the dynamic conditions. It is however possible to derive pseudo-electron density variations at the shortest time-resolution - the pre-integration interval

at which the original data was recorded. This is done by scaling and range-correcting the total power returned from the ionosphere in each range gate. i.e.

$$N_e' = a \times P_R \times R^2 / P_T$$

where  $P_R$  is the returned power, (the zero-lag of the acf),  $P_T$  is the transmitted power,  $R$  is the range and  $a$  is a scaling factor, chosen to give a value of  $N_e'$  in agreement with an ionogram. The true value of electron density is

$$N_e = a' \times P_R \times R^2 (1 + \alpha^2) (1 + T_e/T_i + \alpha^2) / P_T$$

which reduces to

$$N_e = a'' \times P_R \times R^2 (1 + T_e/T_i) / P_T$$

when  $\alpha = \frac{4\pi D}{\lambda} \ll 1$ , i.e. when the radar wavelength  $\lambda$  (at EISCAT 32 cm) is much greater than the Debye length ( $D$ ), typically 0.3 - 4 cm in the F-region. So, as long as  $T_e/T_i$  does not vary  $N_e'$  is an accurate measure of  $N_e$ . We are interested in small spatial-scale variations in  $N_e$  and it is hoped that  $T_e/T_i$  will not vary much, in many of the situations we are interested in. In practice  $T_e/T_i$  may vary, particularly during precipitation so that variations in  $N_e'$  must be checked against the incoherent scatter spectra for evidence of changes in  $T_e/T_i$  before it can be certain whether true electron density variations have been detected.

It has been found that there are large statistical fluctuations in the measurements of 'background' radio-noise and in the measurements of the transmitted power. Measurements of the signal-plus-background returned from the ionosphere would normally be corrected for these two effects using the background and power logged at exactly the same time. However, statistical peaks or troughs in either will result in artificial troughs or peaks in the reduced signal, simultaneously for all ranges from which signal has been received, resulting in apparent field-aligned irregularities (the

beam here being directed parallel to the magnetic field). This means that analysis techniques have had to be adapted to smooth out these variations before reduction. There are also frequent 'spikes' in the recorded signal, sometimes in all range gates, sometimes in only one or two. A computer algorithm is used to delete data at times corresponding to spikes, as they are usually due to satellite echoes or instrumental faults. Some such spikes, however, do seem to contain real information about the ionosphere, in that the shape of the spectrum of the scattered signal is not particularly unusual, and it may simply contain more power. However, it is impractical to check the spectral shape when clearing spikes from the very large volume of data used for the high-time-resolution variation studies, so these are usually deleted along with the rest. The problem of possible variations in receiver gain or in the relative powers transmitted at different frequencies in a multi-frequency experiment, described in the preceeding section, also apply to this method of data reduction.

### Scientific Results

#### Lancaster University Special Programs

The runs of our special program on 17 December 1981 and 3 June 1982 have to be considered as test runs, no ionospheric electron density irregularities having been resolved. This was mainly a result of scheduling constraints which meant that the required conditions (ambient electron density around 300 km height  $> 3 \times 10^{11}$ ; to give adequate signal-to-noise, moderately high magnetic activity and a mid-night time slot, to give a good chance of irregular structure being present) were not satisfied.

The 17 December 1981 run was made in late afternoon, with very quiet magnetic conditions. The available transmitter power was only 500 kW, with a 3% duty cycle, but with the fairly high electron densities present, the uncertainties in the measurement of electron density of 3-6%, although larger than the amplitudes we would expect for small-scale (a few kilometers

or smaller) irregularities, should have been good enough to see any larger scale features. However, none were seen.

The 3 June 1981 run was made with moderately active magnetic conditions but near noon, when most irregular structure is generally found at higher latitudes. Higher power  $\sim 1$  MW was available, along with a 6% duty cycle, but the peak electron density was not very high. The measurement uncertainty of 2-3% should have allowed us to see some larger scale structure, but, again, apparently none was present (Fig.4).

The data from these runs has, however, been useful in development of methods of analysis, as described above.

This early data also showed up several shortcomings in the EISCAT system, some of which have been corrected. The transmitter power and pointing directions were not effectively logged initially; the antennae were taking rather a long (and variable) time to respond to pointing instructions; data was being lost at irregular intervals. Of these, only the pointing direction logging has been fully corrected. Problems still remain with the others, but their effects can be minimized in operations.

The more recent run of our program, on 29/30 November 1982, 2115-0036 UT, was more successful. The experiment was run at night, with a high level of magnetic activity immediately beforehand. Peak electron densities were moderately high ( $\sim 5 \times 10^{11} \text{m}^{-3}$ ) and although the transmitter power was limited to 800 kW, the high duty cycle (10%) meant that a measurement accuracy of 1-2% in electron density could be hoped for. Considerable spread-F was visible on the ionograms so that irregular structure was certainly present.

Analysis of this data is not complete but some qualitative remarks can be made. All the data has been reduced to the pseudo-electron density (range-corrected-power) form, as described above, at the basic integration interval of 4 seconds. This is plotted in Figure 5. For the six,

eight-minute periods when the radar beam was held fixed, parallel to the magnetic field over Tromsø, the data have been integrated and a full-analysis attempted. The results of this analysis for the first three periods have already been shown in Figure 1. During the 4th and 6th periods (2300-2308 and 0028-0036) there were receiver failures, the 5th (2344-2352) is very similar to the 3rd. The electron densities have not been accurately calibrated in an absolute sense as the ionogram was totally absorbed between 2100 and 2300, and the F echo was both range and frequency spread after this time until the experiment ended. Their absolute values may be up to a factor of 1.5 too high or low, but the relative accuracy is  $\sim 2\%$ . The problems outlined above concerning inaccuracies introduced by changes in the relative proportions of the total power being transmitted in the three different-frequency pulses are not likely to affect this data seriously. The power has been averaged over three of the four frequencies transmitted, the fourth being a short pulse, on average containing only 6.25% of the total power, so that a change in the relative power in this pulse by even as much as 30%, would change the power in the other three by less than 2%.

Figure 6 shows the horizontal components of the ion drift velocity, derived for each of the six periods when the beam was held stationary. Figure 7 illustrates the effective path of the radar beam through the ionosphere, at 300 km altitude, during the scanning sequences, taking into account both the measured plasma drift and the beam scanning. The intention of this experiment was to scan backwards and forwards through a fairly small region of the ionosphere but, because of the rapid drift in the earlier half of the experiment, this may have been achieved only in one sequence, the elevation scans from 2308-2344. Because of the very large uncertainties in determining the plasma drift, however, we cannot be sure we achieved our aim even then! During most of the experiment the beam moved, effectively,

continually northward, and westward or eastward. Examination of Figure 5 shows that during this northward migration the beam passed from a region with some structure in the lower F-region, and low peak electron densities (2115-2123), through a region with much higher electron densities and large-amplitude structures (up to 100%  $N_e$  enhancement, 2123-2158), then through a less structured F-region, still with rather high peak electron densities and with higher densities at the lowest altitudes (2158-2225). Moderate amplitude ( $\sim 50\%$ ) structure is again seen during the (possible) N-S scanning sequences from 2300-2340, with little structure seen thereafter.

The structures appear to be field aligned, with variations with range in the time of observation being explicable by the inclination of the beam away from the field-parallel direction. The structures appear to be of two types, either with large amplitudes at the lowest ranges observed, decreasing in amplitude with height until they disappear before reaching  $\sim 500$  km altitude, or with large amplitudes at and above the F-peak, decreasing in amplitude downwards and disappearing below 250 km altitude.

To summarise, large amplitude, field-aligned structures, on scale sizes  $\sim 10$  km are clearly present. However faster scanning of the radar antenna will be needed when large ionospheric drifts are present, and much better resolution of these drifts is needed before we can attempt to map the 3-D shape of these structures in detail.

#### Common Program Measurements

Common program data for a few hours either side of magnetic midnight, on 7 October 1981 have been analysed in detail. The results are illustrated by Figure 8 (standard reduced parameters), Figure 9 (range corrected power), and Figure 10 (horizontal drift). On this occasion program CPM1 was running, i.e. measurements were made with the radar beam pointing parallel to the magnetic field at 300 km altitude, with the remote sites making measurements in sequence in the E-region, at 300 km and at 700 km. This was a very active

19.

night (local K index 7, 5 for the time period shown) and the electron densities (calibrated to an ionosonde reading at 2100) reach high values ( $>10^{12}$ ).

The electron density plot in Figure 8 shows that there are large fluctuations in electron density as the plasma drifts through the beam, with densities rising by 100% on occasion, in the space of a few minutes. The horizontal drifts are around 500-1000 m/s between 1900 and 2300, when these large variations are seen, so that, for example, the enhanced density regions seen for about half an hour have scale sizes of the order 1000-2000 km. The time resolution of this data is 2½ minutes so the smallest scale sizes resolvable are around 150-300 km.

If the  $N_e$ ,  $T_e$ ,  $T_i$  and  $V_i$  plots are considered together several features stand out. There is a pronounced minimum in  $T_e$  which coincides with the isolated electron density enhancement centred at 2300; this could result from the increased electron heat-loss rate in a region of enhanced ionisation, if this enhanced region was formed some time previously. There are maxima in  $N_e$  and  $T_e$ , throughout the F-region, associated with increases in E-region electron density and with very little, or no, increase in  $T_i$  at ~ 1830, 2030 and 2215: these features suggest particle precipitation. Other features such as the pronounced increase in ion temperatures at ~ 2240 and the sharp increase in outward ion flow (minimum on plot) at 2330, which occurs just as electron densities fall to much lower values (where they remain for the next several hours) are also worth noting, but as they do not directly concern F-region structure, we will not consider them further here.

In order to look at the smaller scale structuring, the range-corrected power has been plotted (Figure 9). This is available at 15 seconds time resolution, allowing us to look at scale sizes of about 15-30 km. These plots show frequent very rapid, spiky, enhancements which had been smoothed out by the post-integration necessary to make the full analysis. Where these very



short features seem not to be associated with precipitation, i.e. where the E-region is not involved, at 1950, 2040, 2107, 2114, 2205, 2226, 2300 and 2315 they are generally associated with larger-scale gradients (with the exception of the feature at 2114). If we think of the electron density enhancements as localized regions in space drifting through the beam, then the very rapid electron density variations occur on the receding walls of the enhancements from 2040 onwards, and on the approaching wall at 1950. The horizontal drift shown in Figure 10 shows that these probably correspond to the western wall, from 2040 onwards and to the equatorward wall at 1950.

A possible structuring mechanism seems to be the  $\underline{E} \times \underline{B}$  gradient drift instability. In order to check whether this might be applicable we need to know the velocity of the plasma relative to the neutral air. We can derive the meridional component of the neutral air velocity from the plasma velocity parallel to the magnetic field, which is

$$V_{i||} = V_n \cos I + \frac{\sin I (\partial N (T_i + T_e) / \partial h + N m_i g)}{N m_i \nu_{in}}$$

where  $V_n$  is the horizontal, meridional neutral wind,  $I$  is the magnetic inclination, and the other term represents ambipolar diffusion parallel to the field, caused by gravity and the plasma pressure gradient.  $V_{i||}$  and the altitude variations of  $N_e$ ,  $T_e$  and  $T_i$  are measured using the radar,  $m_i$  is assumed to be 16 a.m.u. (i.e. only oxygen ions are present) and the ion neutral collision frequency  $\nu_{in}$  is estimated as  $\sim 1$  at 300 km altitude (Banks and Kockarts, 1973). The magnetic inclination is taken as  $77.6^\circ$ , and  $g$  at 300 km is  $\sim 9 \text{ m/s}^2$ . The F peak is above 300 km in this time interval and the resultant downward diffusion speeds are around 25-45 m/s. The

derived meridional neutral winds are also plotted in Figure 10. We cannot derive the zonal neutral wind from the incoherent scatter data but this would be small where the zonal ion drift is small, around 1900-2000 and rather larger, due to the effects of ion drag, from 2000 onwards (Fuller-Rowell and Rees, 1980). However, it should still be less than the zonal ion drift. Thus the plasma drift at 1950 is very probably northward, relative to the neutral air, and after 2040, it is mainly eastward. The trailing edge of an electron density enhancement is unstable to the gradient drift instability, i.e. the equatorward edge at 1950, and the western, or south-western edge after 2040. This agrees with the observations (Fig. 11). It appears, therefore, that the  $\underline{E} \times \underline{B}$  gradient drift instability could explain the observed structuring, associated with electron density gradients, at the smallest observable scale sizes.

This is, of course, not a conclusive proof that this mechanism is responsible. Theoretical calculations, for example, have suggested that this mechanism cannot operate if the ambient electric field is not close to orthogonal to the electron density gradient (Huba et al., 1983). More detailed information concerning the exact form of the large-scale structures is needed to determine precisely the directions of the gradients.

To summarize, analysis of a few hours of Common Program data has shown the presence of field-aligned structure in F-region electron density on scale sizes from 30 km to a few thousand kilometres, with regions  $\sim 1000$ -2000 km across having electron densities in their centres as much as twice those at their edges. Smaller structures, with scale sizes  $\sim 30$  km are observed associated with the walls of the large structures, and may have been generated by the  $\underline{E} \times \underline{B}$  gradient drift instability. Further structures with scale sizes  $\sim 30$  km or more are clearly associated with concurrent particle precipitation. Analysis of further Common Program data is underway.

### Conclusions

Considerable progress has been made in the last year in the availability of large volumes of (unprocessed) data, and in the availability of reliable software for deriving ionospheric parameters from that data. Significant problems remain with the derivation of ion drift velocities, and further investigation of this problem must have a high priority.

Further analyses of Common Program data should be made in order to determine whether the association of intermediate-scale structure with large-scale gradients occurs on occasions other than the one shown above, and how often this could be explained by the  $\underline{E} \times \underline{B}$  gradient drift instability. A more detailed study of the F-region electron density variations which evidently occur during precipitation events might also be instructive.

Lastly, it is clear that the rapid-scanning Special Program experiments can resolve small scale structures and, once the accuracy of drift velocity determination is improved, these may provide detailed information on the structure of large and intermediate scale electron-density enhancements.

### Acknowledgements

This research has been sponsored in part by European Office of Aerospace Research and Development. The staff of the U.K. EISCAT group at the Rutherford and Appleton Laboratory, particularly Dr. A.P. Van Eyken, have given advice and support. C.M. Hall gave assistance with software development and data processing. Data was received from the EISCAT Scientific Association, an association of Government funded Research Agencies in six countries (Finland, France, Germany, United Kingdom, Norway, Sweden) responsible for the installation and operation of an incoherent scatter facility in Northern Scandinavia.

### References

- Banks, P.M., Kockarts, G: Aeronomy. New York, London: Academic Press 1973.
- Clark, D.H., Raitt, W.J. The global morphology of irregularities in the topside ionosphere as measured by the total ion current probe on Esro-4. Planet. Space Sci. 24, 873-881, 1976.
- Fejer, B.G., Kelley, M.C. Ionospheric irregularities. Rev. Geophys. Space Phys. 18, 401-454, 1980.
- Fremouw, E.J. and Lansinger, J.M. Dominant configurations of scintillation producing irregularities in the auroral zone. J. Geophys. Res. 86, 10087-10094, 1981.
- Frihagen, J. Irregularities in the electron density of the polar ionosphere. In: The polar ionosphere and magnetospheric processes, G. Skovli, ed: pp. 271-284. New York: Gordon and Breach 1970.
- Fuller-Rowell, T.J., Rees, D. A three-dimensional global model of the thermosphere. J. atmos. Sci., 37, 2545-2565, 1980.
- Huba, J.D., Ossakow, S.L., Satyanarayana, P., Guzdar, P.N.: Linear theory of the  $E \times B$  instability with an inhomogeneous electric field. J. Geophys. Res. 88, 425-434, 1983.
- Kelley, M.C., Vickrey, J.F., Carlson, C.W., Torbert, R. On the origin and spatial extent of high-latitude F-region irregularities. J. Geophys. Res., 4469-4475, 1982.
- Livingston, R.C., Rino, C.L., Owen, J., Tsunoda, R.T.: The anisotropy of high-latitude nighttime F region irregularities. J. Geophys. Res. 87, 10519-10526, 1982.
- Phelps, A.D.R., Sagalyn, R.C. Plasma density irregularities in the high latitude topside ionosphere. J. Geophys. Res. 81, 515-523, 1976.
- Rino, C.L., Vickrey, J.F.: Recent results in auroral-zone scintillation studies. J. Atmos. Terr. Phys. 44, 875-887, 1982.

- Sandford, B.P. Optical emission over the polar cap. In: The polar ionosphere and magnetospheric processes, G. Skovli, ed. : pp.299-321. New York: Gordon and Breach 1970.
- Vickrey, J.F., Kelley, M.C. The effects of a conducting E layer on classical F-region cross-field plasma diffusion. J. Geophys. Res., 4461-4468, 1982.

## Figure Captions

Fig. 1. Profiles of average electron density,  $N_e$ , ion and electron temperature,  $T_i$  and  $T_e$  and ion drift  $V_i$  for the three time intervals indicated on 29 November 1982. Measurements were made using the EISCAT radar with the transmitted beam directed parallel to the magnetic field at 300 km altitude at Tromsø. The numbers 1, 2 and 3 refer to the measurements made using three different transmitting frequencies, 933.5, 934.0 and 934.5 MHz, respectively. The error bars are the uncertainties estimated by the parameter-fitting routines (see text).

Fig. 2. Scatter plots of differences between parameter estimates made using different radar frequencies ( $\sigma_m$ ) and uncertainties in the differences expected from those calculated by the parameter-fitting routines ( $\sigma_c$ ). Plots are for  $T_e$ ,  $T_i$  and  $V_i$ , as indicated.

Fig. 3. Histogram of differences in velocities between measurements for radar frequency 3, and frequency 1 or 2. An artificial doppler-shift was introduced in the receiver chain for frequency 3, corresponding to a velocity shift of 320 m/s. The solid line is for well-estimated velocities, the dashed line for less-good estimates (see text).

Fig. 4. Pseudo-electron density variations in four elevation scans recorded 1200-1230 on 3 June 1982.

Fig. 5. Pseudo-electron density variations during scanning sequences 2115-0036 on 29/30 November 1982. Letters a-v correspond to the labels on segments of the "effective path" illustrated in Figure 7.

Fig. 6. Horizontal ion drift at 300 km altitude above Tromso on 29/30 November 1982.

Fig. 7. Effective path of radar beam through the ionosphere during scanning sequences on 29/30 November 1982, taking into account the plasma drift shown in Fig. 6. Segments a, f, k, l, q, v are with the beam pointing in a fixed direction; b-e, m-p are elevation scans; g-j, r-u are azimuth scans. The solid lines are the most probable paths, the dashed lines indicate the effect of uncertainties in drift velocity determination.

Fig. 8.  $N_e$ ,  $T_e$ ,  $T_i$  and  $V_i$  variations 1800-2400 UT on 7 October 1981. Integrated to  $2\frac{1}{2}$  minutes time resolution, fitted with compositions fixed to model values.

Fig. 9. Pseudo-electron density at 15 seconds time resolution 1800-2400 UT on 7 October 1981. The first plot has the same time scale as Fig. 8, for comparison. The other plots have expanded time scales,  $\sim 1$  hour per plot.

Fig. 10.  $\underline{E} \times \underline{B}$  ion drift and meridional neutral wind,  $V_n$ , at 300 km altitude above Tromso. Because the sign of the drift-component measured by the Kiruna receiver is uncertain either of the two velocity distributions may be the correct one. For the derivation of  $V_n$ , see text.

Fig. 11. Pseudo electron density variations at the F-peak, plotted as N-S and E-W variations, and explanation of the 'spiky' structures as  $\underline{E} \times \underline{B}$  gradient-drift instabilities (see text).

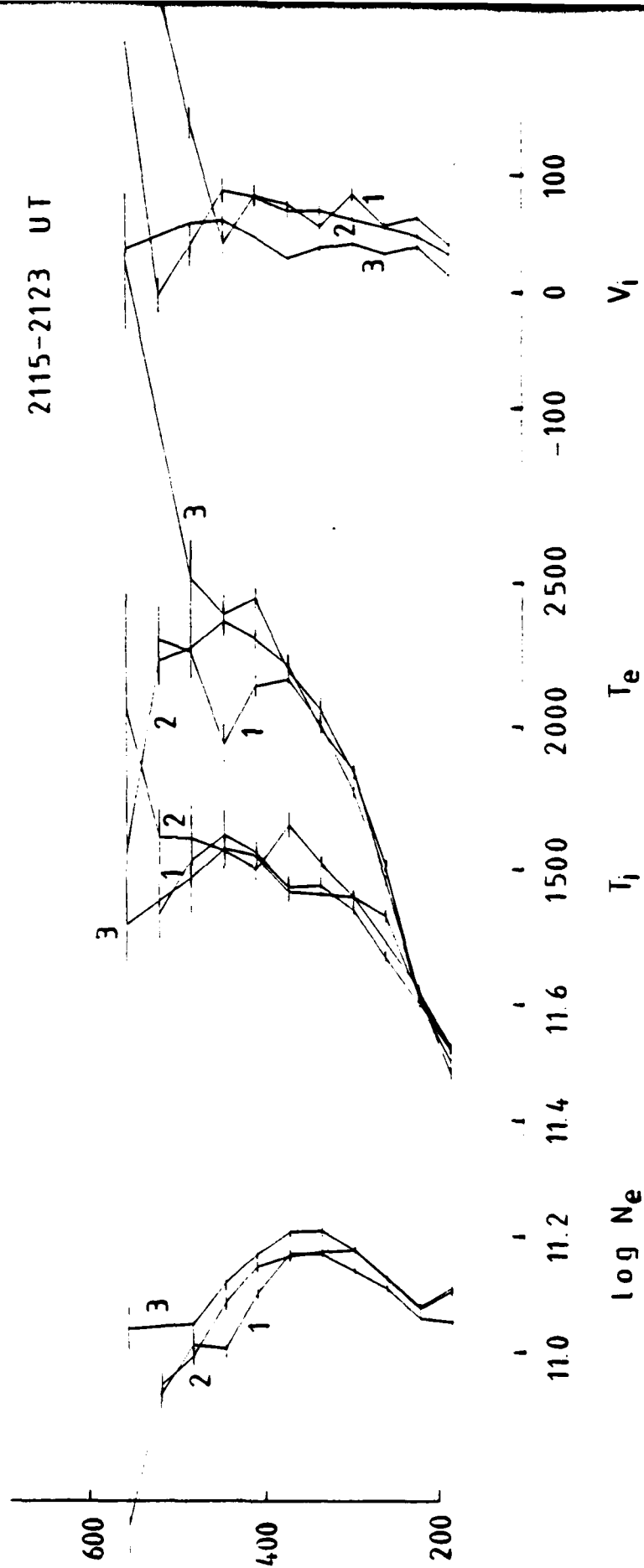


Figure 1a



2159-2207 UT

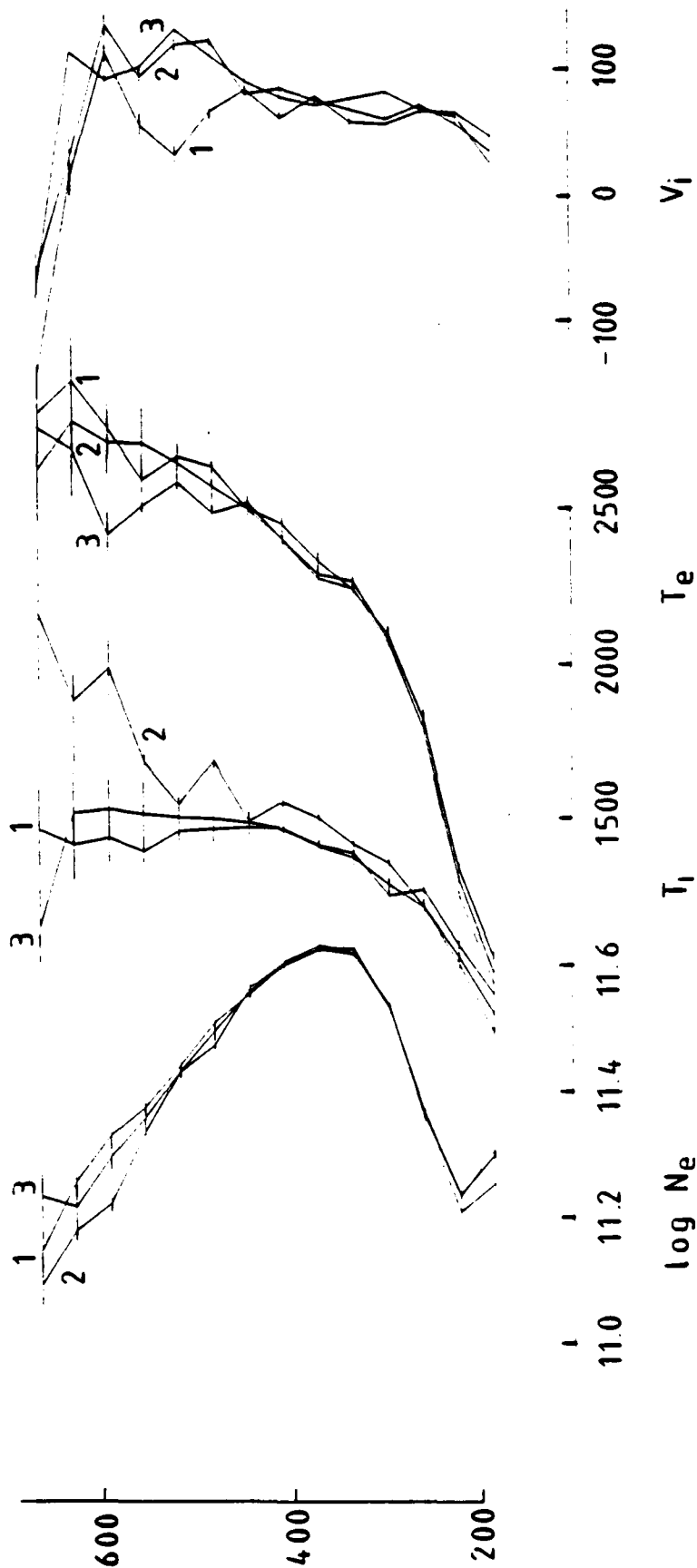


Figure 1b

2243-2251 UT

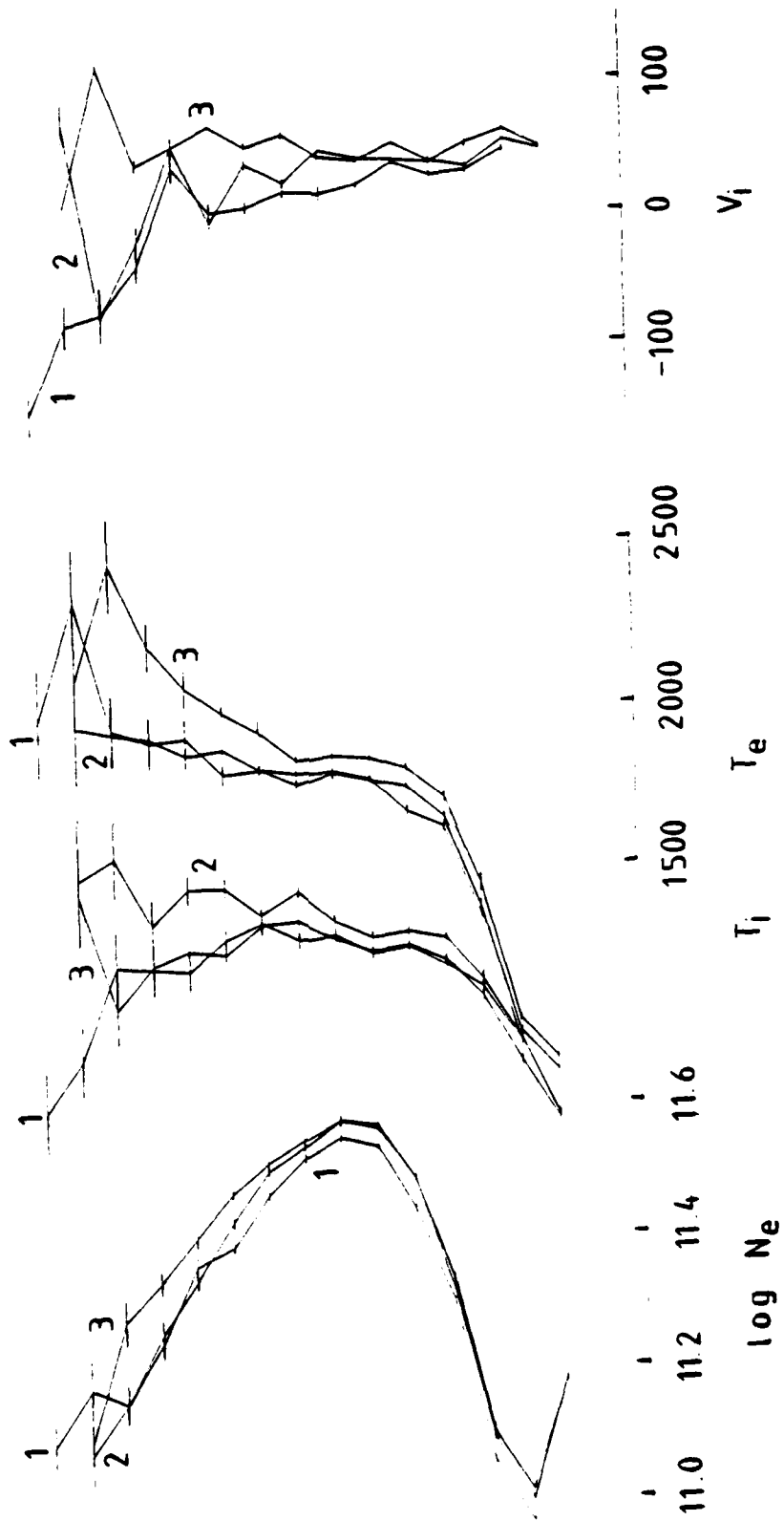


Figure 1c

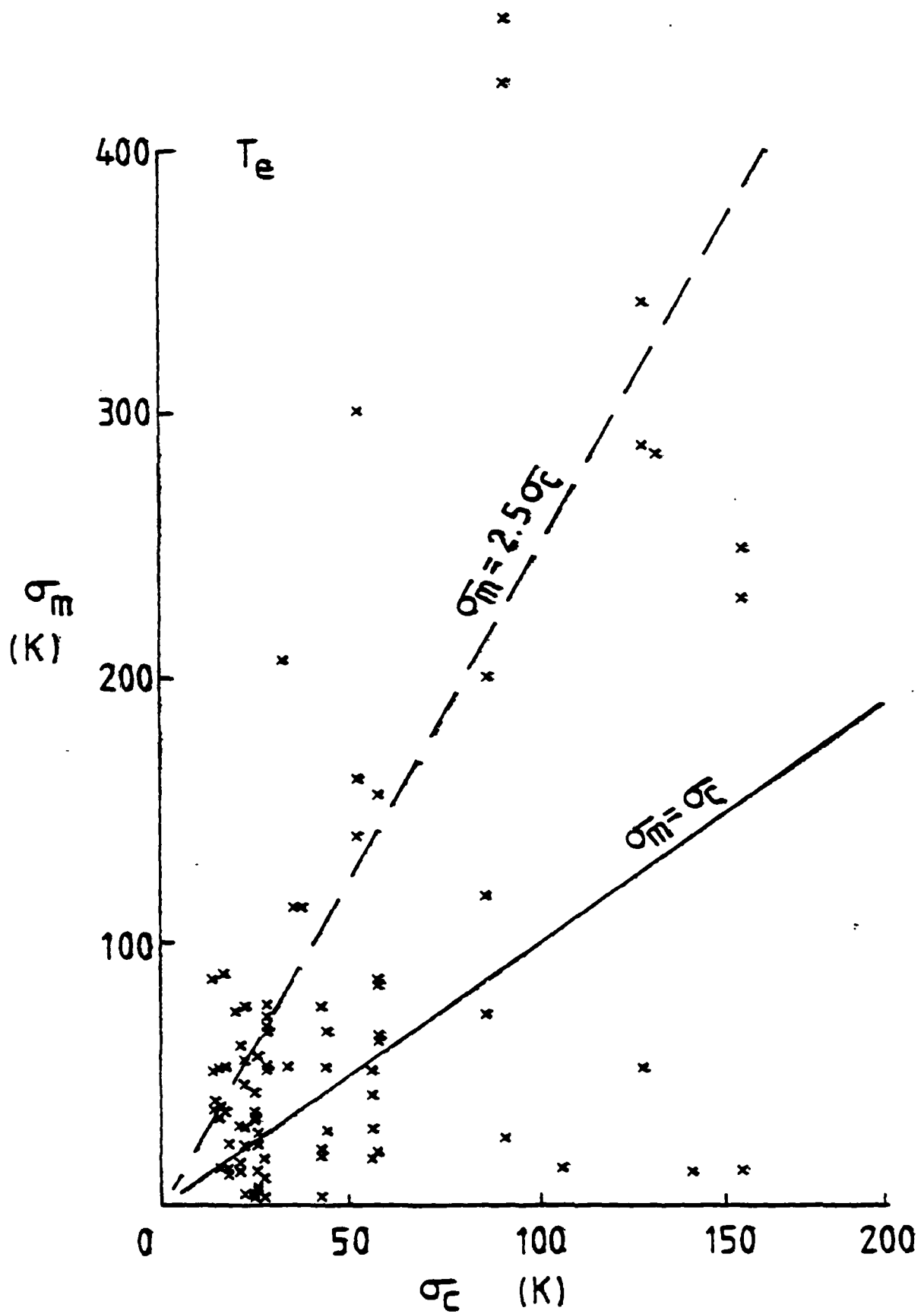


Figure 2a

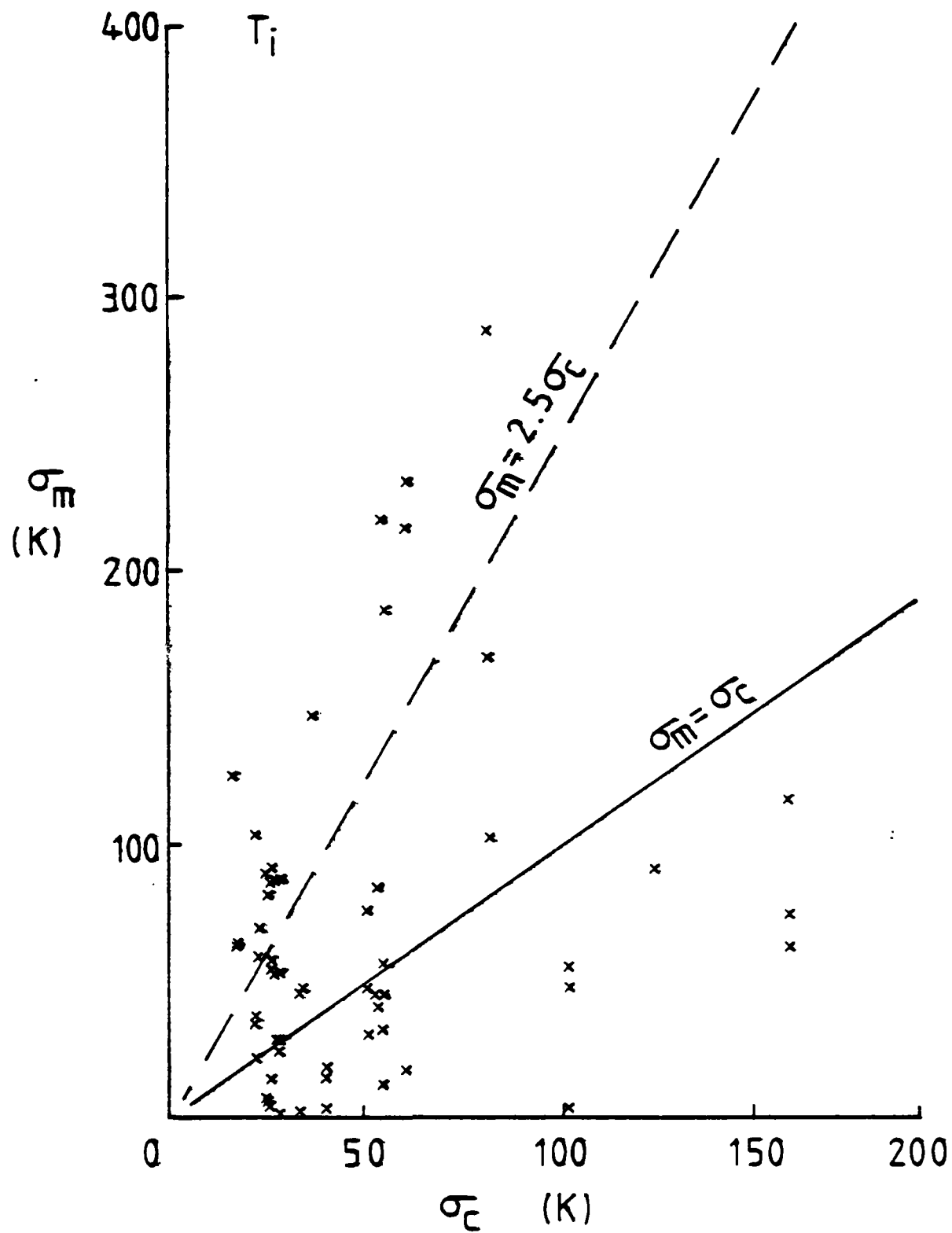


Figure 2b

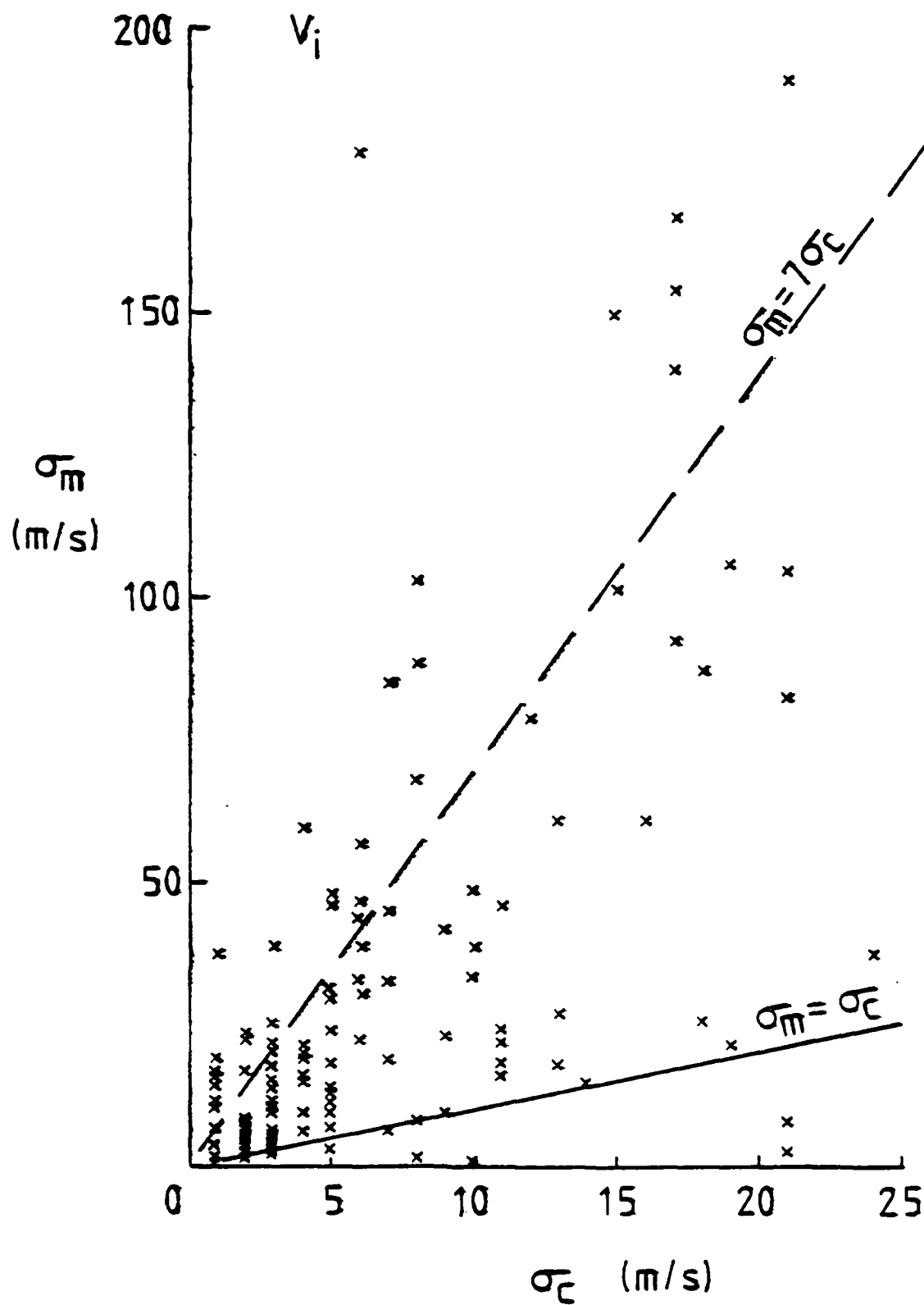


Figure 2c

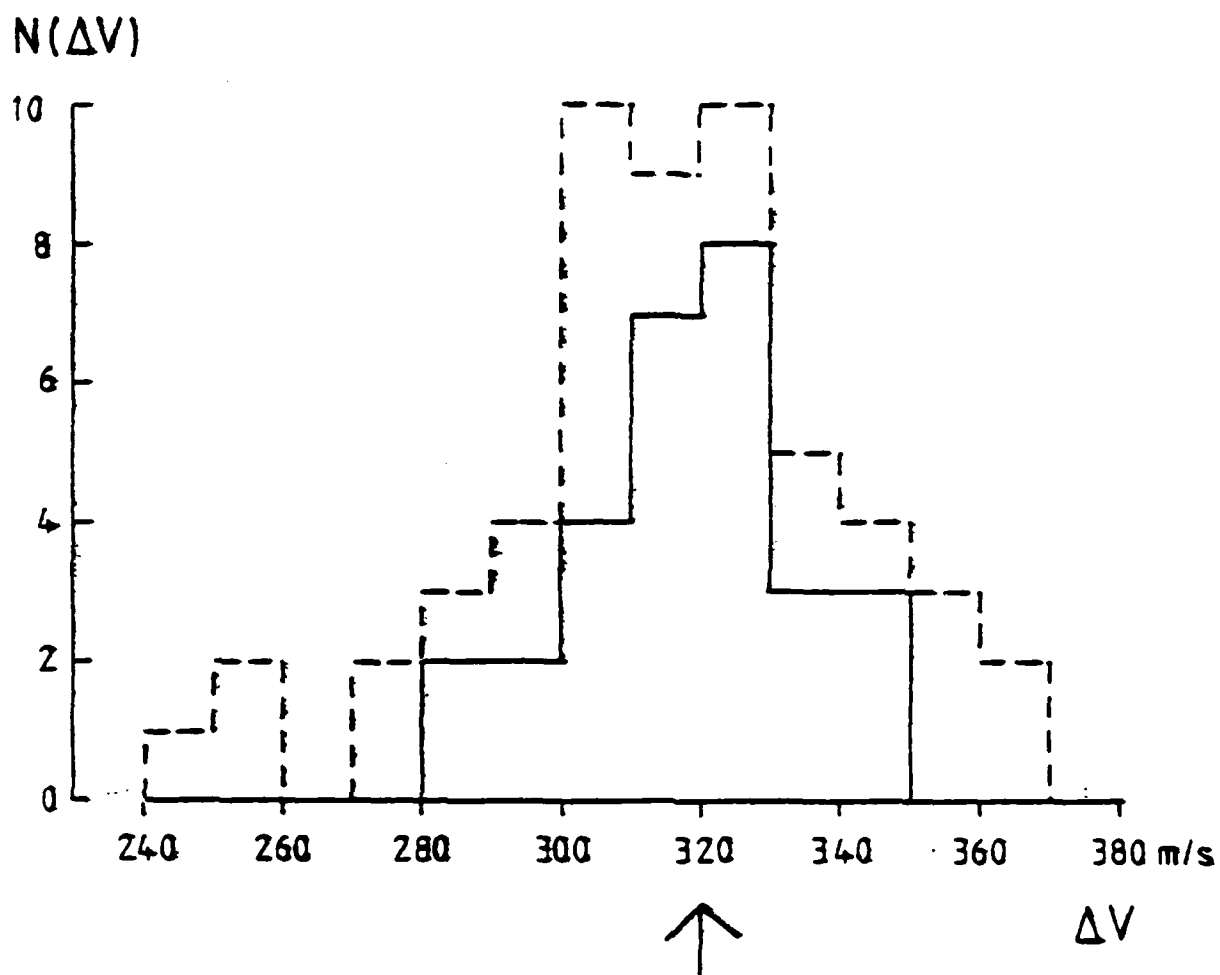
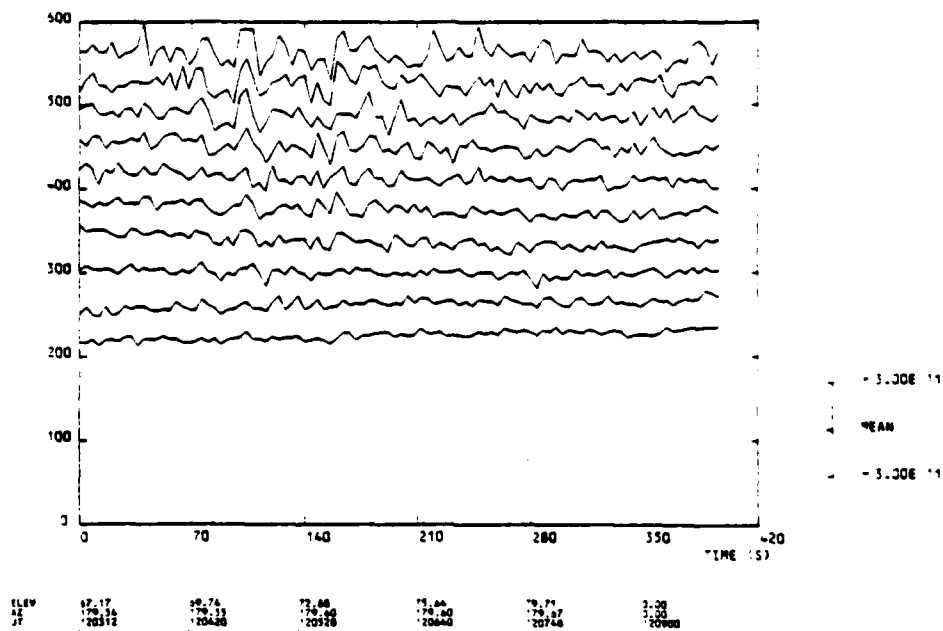


Figure 3

EISCAT TROMSO

ELECTRON DENSITY

03 JUN 1982 SKSP1



EISCAT TROMSO

ELECTRON DENSITY

03 JUN 1982 SKSP1

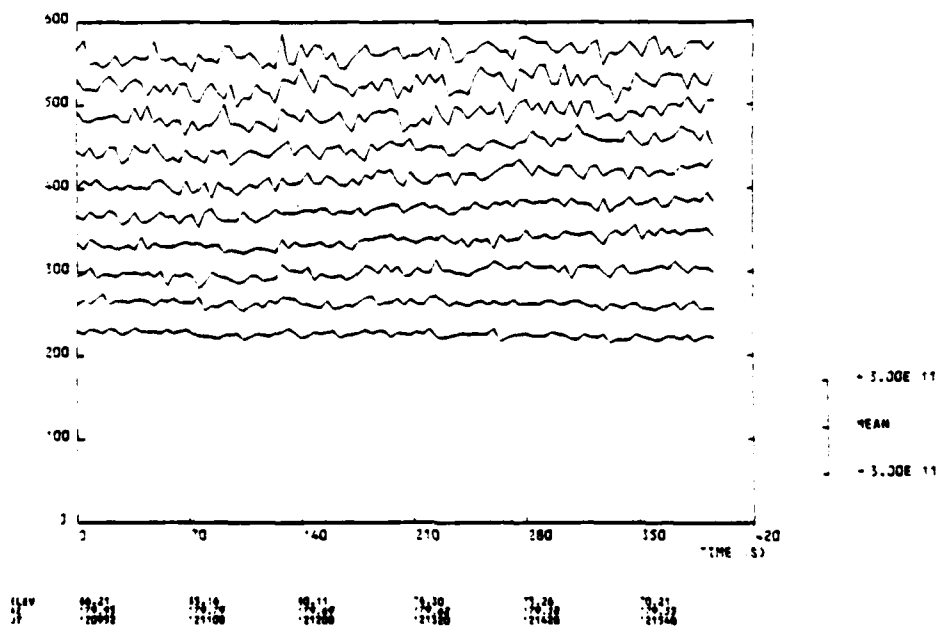


Figure 4a





FISCAL PROMISO ELECTRON DENSITY 29 NOV 1982

RANGE CORR POWER

MEAN VALUE

RANGE

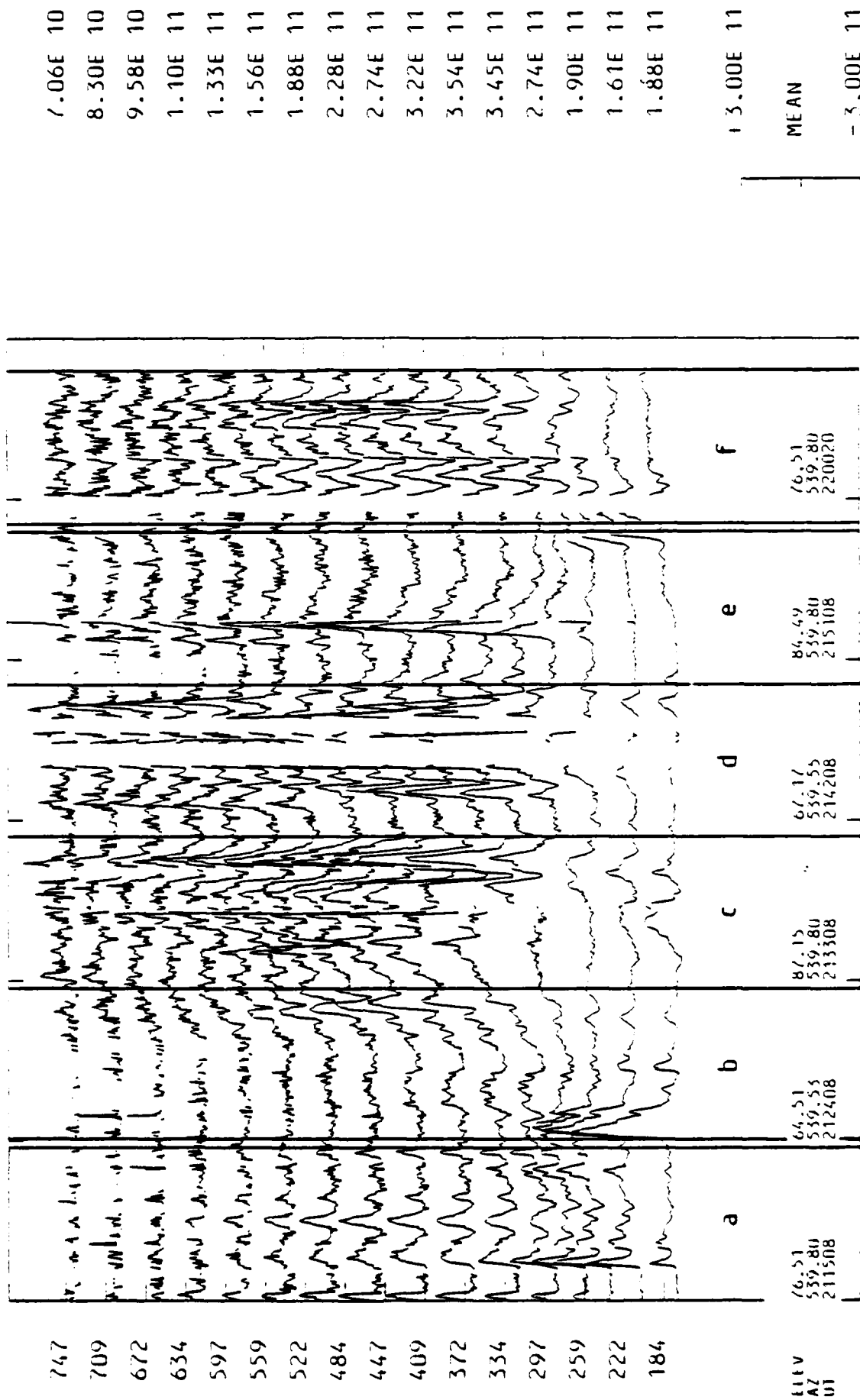


Figure 5a

1 ESCAL FROM 50

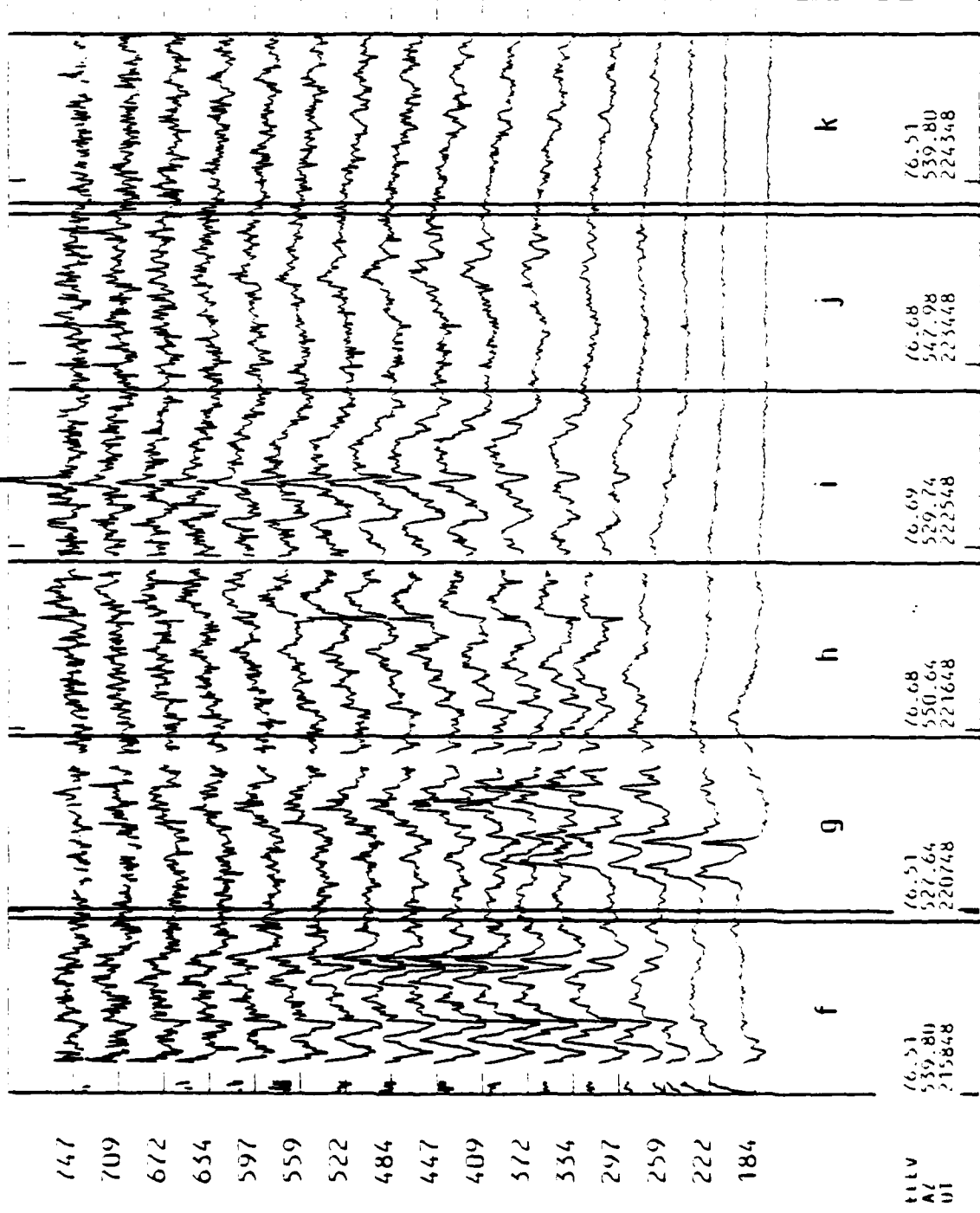
ELICIRON DENSITY

29 NOV 1982

RANGE CORR POWER

MEAN VALUE

RANGE



8.20E 10

9.94E 10

1.25E 11

1.54E 11

1.91E 11

2.32E 11

2.80E 11

3.31E 11

3.80E 11

4.16E 11

4.31E 11

4.05E 11

3.54E 11

2.23E 11

1.64E 11

2.01E 11

13.00E 11

MEAN

-3.00E 11

Figure 5b

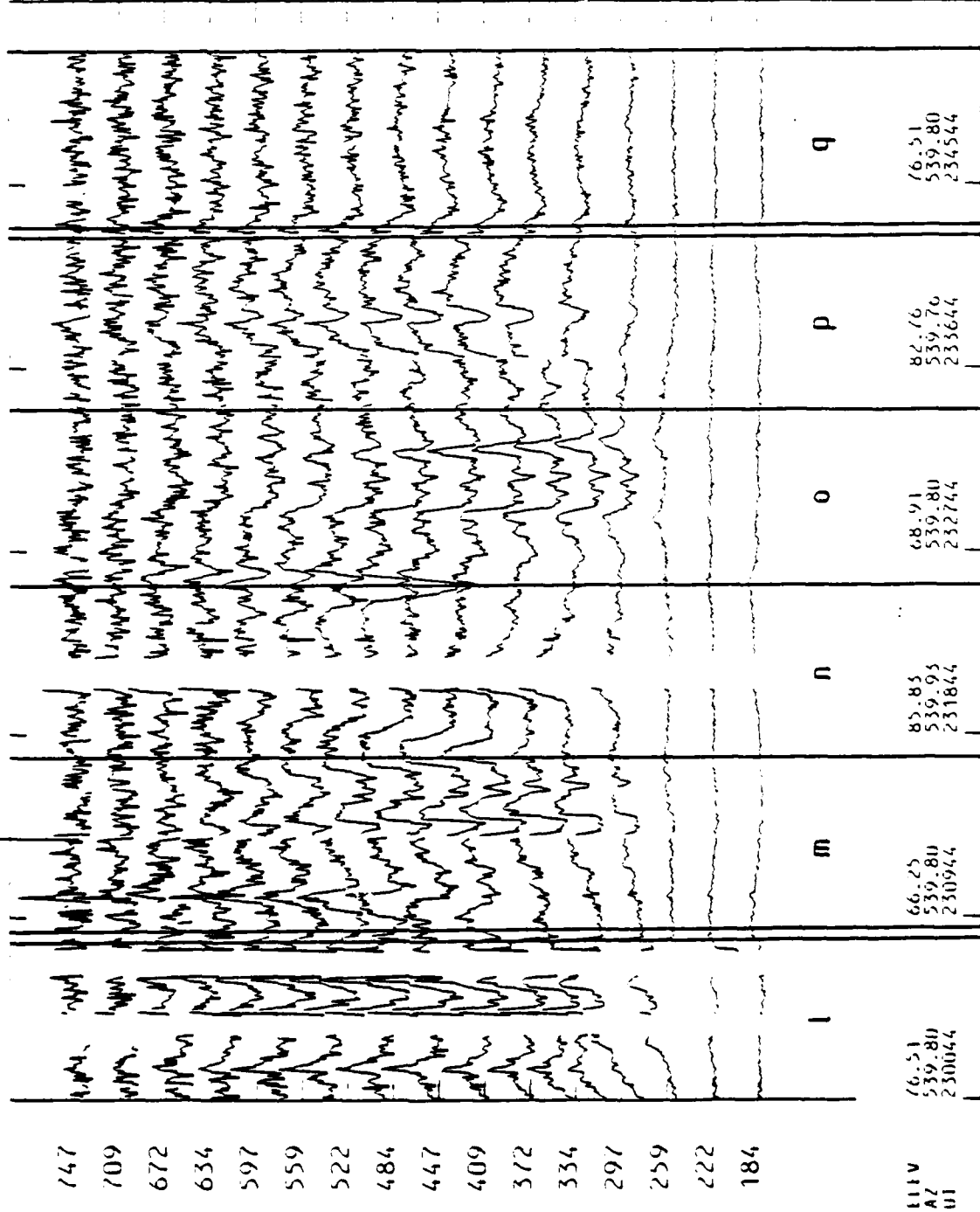
FISCAL FROM 50

ELECTRON DENSITY  
RANGE CORR POWER

29 NOV 198

RANGE

MEAN VALUE



111V  
AZ  
UI

+ 3.00E 11

MEAN

- 5.00E 11

TIME (S)

Figure 6.

# ELSCA FROM SO ELECTRON DENSITY RANGE CORR POWER

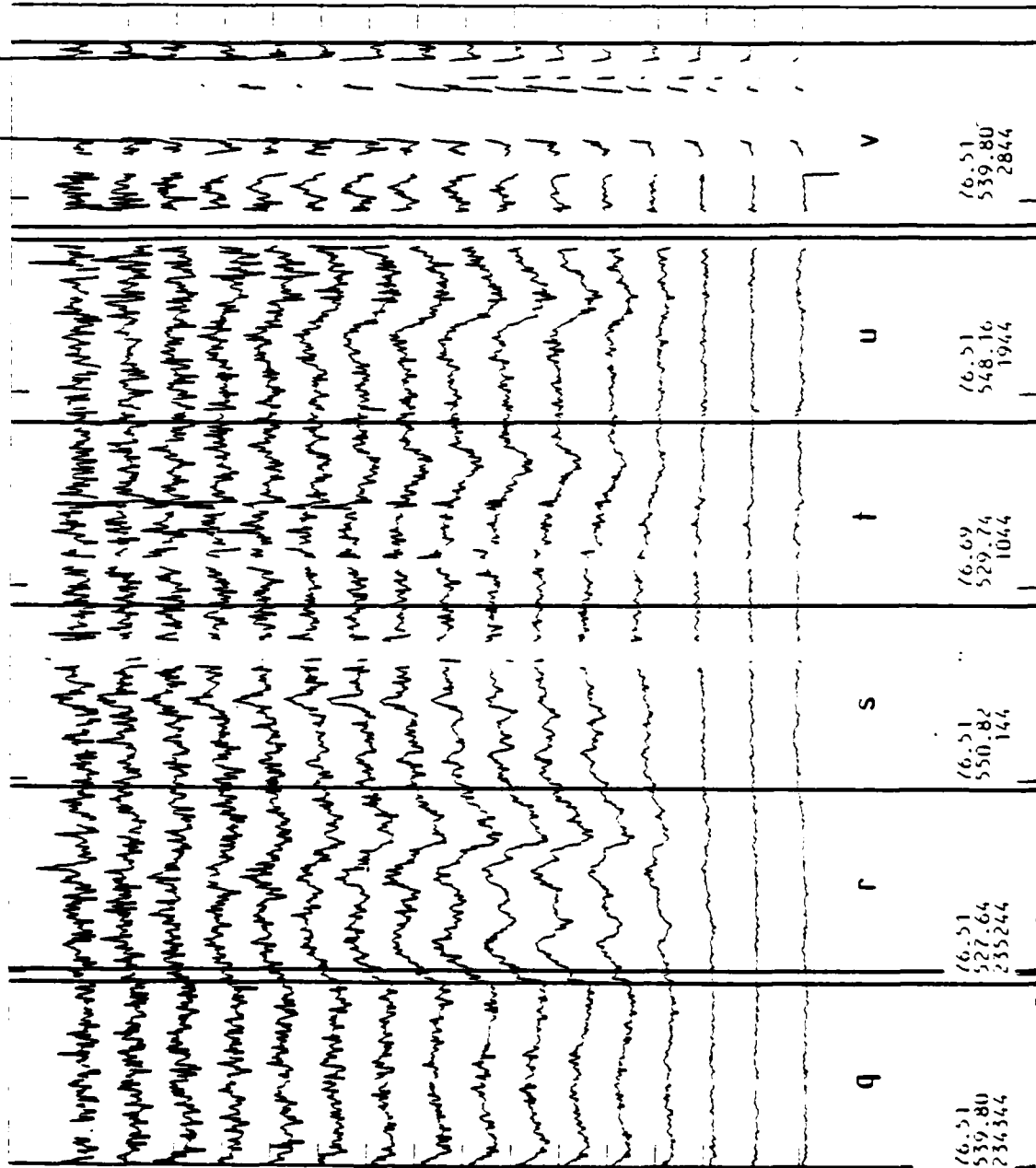
29 NOV 198

RANGE

MEAN VALUE

747  
709  
672  
634  
597  
559  
522  
484  
447  
409  
372  
334  
297  
259  
222  
184

9.47E 10  
1.17E 11  
1.46E 11  
1.83E 11  
2.30E 11  
2.83E 11  
3.43E 11  
4.03E 11  
4.58E 11  
4.84E 11  
4.63E 11  
3.83E 11  
2.57E 11  
1.49E 11  
1.30E 11  
1.73E 11



EL EV  
A Z  
UI

76.51  
539.80  
2844

76.51  
548.16  
1944

76.69  
529.74  
1044

76.51  
550.82  
144

76.51  
527.64  
255244

+ 5.00E 11

MEAN

- 3.00E 11

TIME (S)

Figure 5d

29 Nov 1982

2100  
|

2200  
|

2300  
|

2400  
|

0100 UT  
|



---

500 m/s

Figure 6

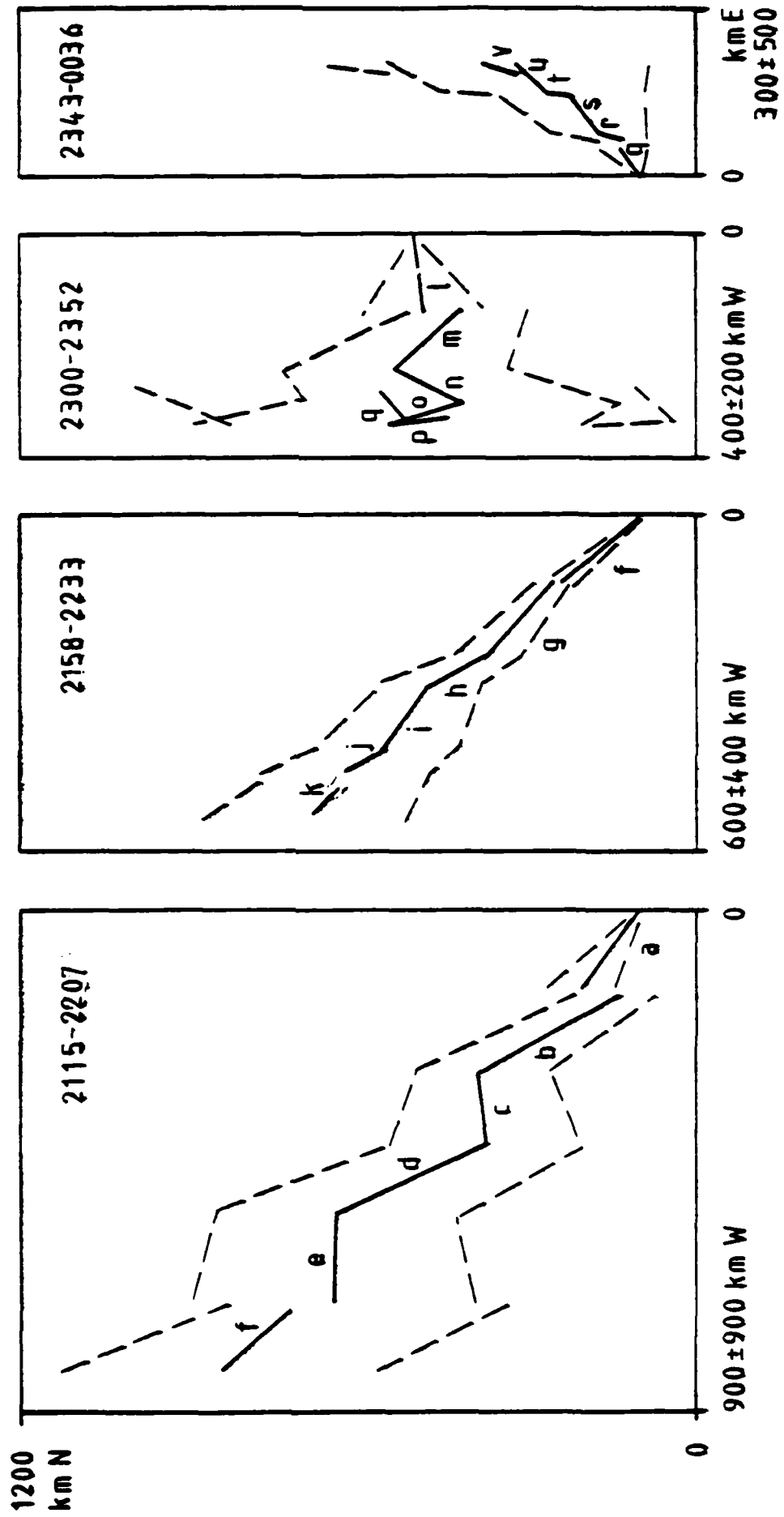


Figure 1









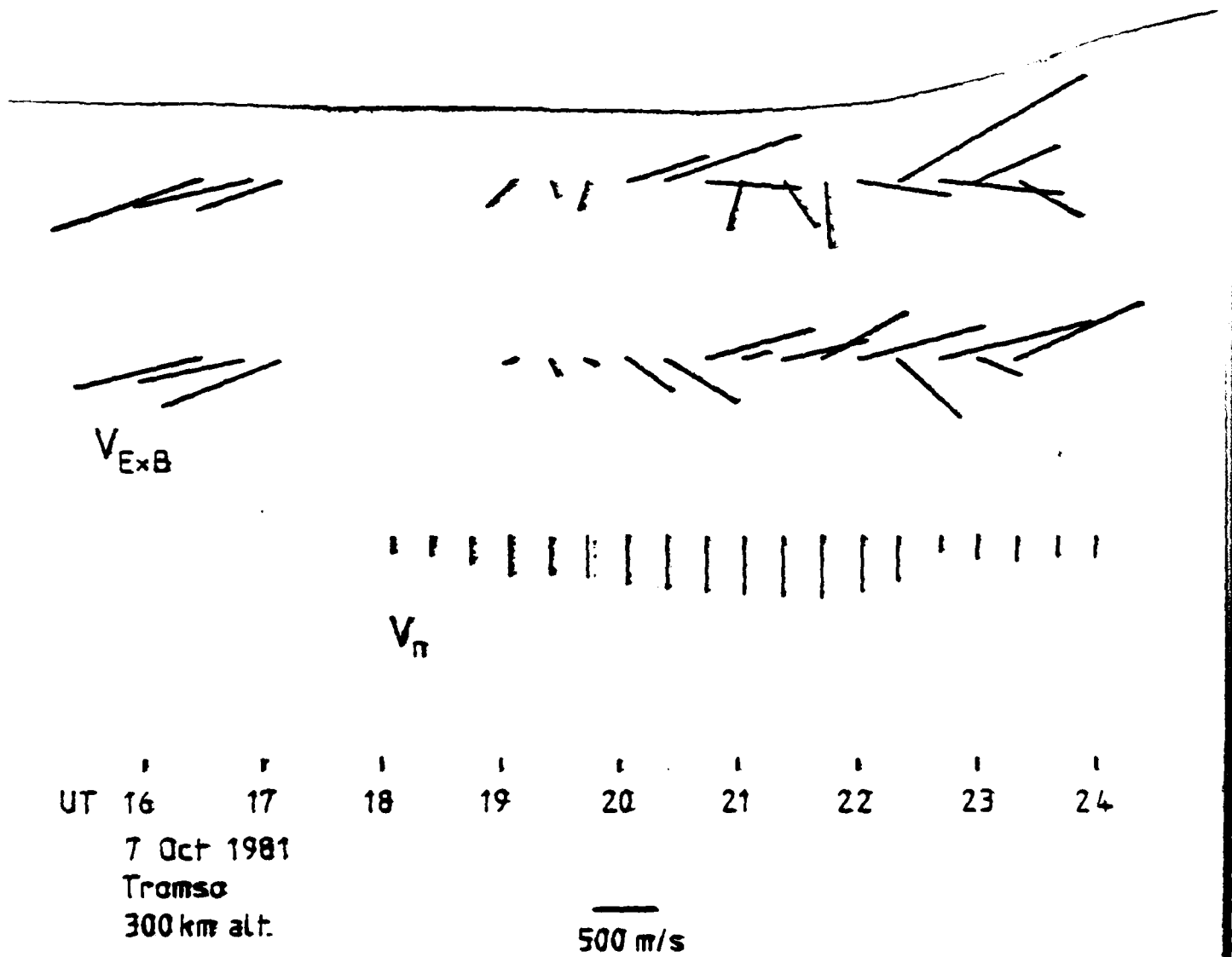


Figure 10

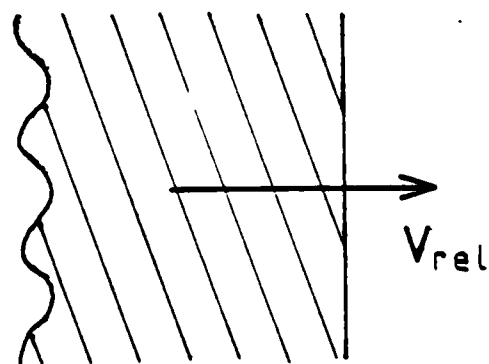
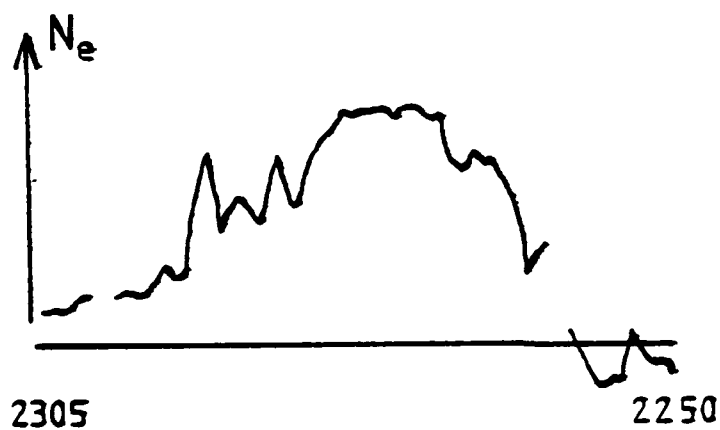
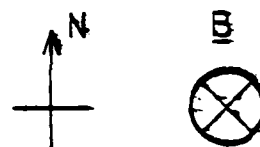
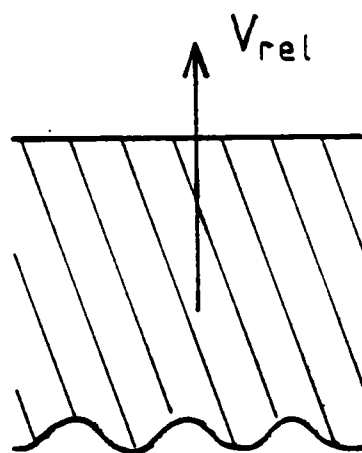
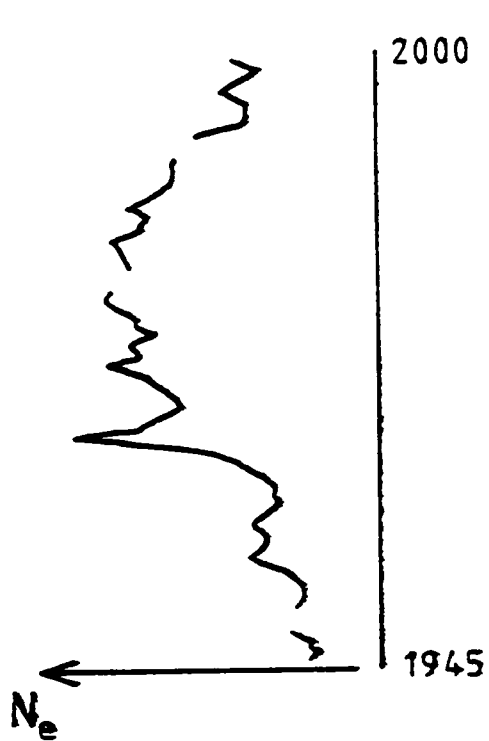


Figure 11

**DAT  
FILM**